JOURNAL OF APPLIED ELECTROCHEMISTRY 4 (1974) 337–345

Electrochemical behaviour of iron in alkaline sulphate solutions

D. GEANA*, A. A. EL MILIGY and W. J. LORENZ

Institute of Physical Chemistry and Electrochemistry, University of Karlsruhe, Karlsruhe, Germany

Received 4 May 1974

The electrochemical behaviour of pure iron in alkaline sulphate solutions was studied using cyclic voltammetry at $T = 298$ K. It has been found that the results depend on the polarization pre-treatment of the electrode and the activation state of its surface. At starting potentials in the range of hydrogen evolution and at maximum activation conditions, the voltammograms show three anodic current maxima and two cathodic ones. A correlation between these different maxima is given. The electrode processes, which may take place at these maxima, are discussed in terms of possible iron dissolution mechanisms.

1. Introduction

The investigations carried out on the electrochemical behaviour of iron in alkaline solutions are relatively few compared to those done in acid solutions. This type of investigation is, however, important from the technical point of view, e.g.

(a) Technology of alkaline Fe–Ni accumulator [1] as well as Fe–air battery [2].
(b) electrochemical manufacture of oxide films, which find an important application in electronics [3] and
(c) corrosion of iron and steels and their protection as in the case of nuclear reactor technology [4].

Kabanov *et al.* [5] studied the kinetics of iron in sodium hydroxide solution using the galvanostatic method. They suggested the formation of $Fe(OH)_2$ and $Fe(OH)_3$ and presented a mechanism. Further, Weil [6] and Hurlen [7] investigated the same system using different electrochemical techniques. Physical methods, namely X-ray and electron diffraction, were used by Salkind *et al.* [8] and Foley *et al.* [9] in order to determine the type of iron oxides formed in these alkaline media. Schephard and Schuldiner [10] have shown that steady state measurements on iron in alkaline media are relatively difficult. Therefore, some other authors [11–15] used non-steady state techniques, e.g. cyclic voltammetry and galvanostatic and potentiostatic pulse measurements. Asakura and Nobe [11] for example, investigated the behaviour of iron in potassium hydroxide solution using the potentiostatic single sweep technique. They studied the processes occurring at the electrode surface and their dependence on the starting potential.

Cyclic voltammetry is more suitable than the single sweep method for studying the electrochemical behaviour of iron in alkaline solutions over a wide potential range. This method was used recently for investigating the electrochemistry of iron in hydroxide solutions [14].

The kinetics of iron dissolution in weak acid sulphate solutions in the potential range between the active and the passive state was investigated by Lorenz *et al.* [16] using cyclic voltammetry.

Some of the data obtained in the earlier investigations on the electrochemical behaviour of iron electrodes in alkaline solutions were not completely reproducible and there were also some contradictions due to different interpretations of the measured results [5–15].

Consequently a uniform dissolution mechanism

* Permanent address: Department of Physical Chemistry and Electrochemistry, Polytechnic Institute of Bucharest, Romania

could not be deduced. However, the authors agree that OH^- ions stimulate the active dissolution process and participate in the formation of different hydroxides as well as oxides on the electrode surface. The composition of the formed oxide layers could be detected experimentally in an independent way by using physical methods. Thus, the existence of γ–Fe_2O_3 and Fe_3O_4 at relatively high anodic potentials was confirmed [8, 9]. It was not possible to present a definite mechanism of iron dissolution and oxide layer formation on the electrode surface in alkaline media, due to the following difficulties:

(1) In the potential range of the active iron dissolution the degree of coverage of the electrode surface with the intermediate $(FeOH)_{ads}$ is large. Therefore consecutive reactions leading to hydroxides and oxides can take place preferentially.

(2) The kinetics of electrode processes with parallel and consecutive steps including the specific adsorption of different intermediates as well as the formation of surface oxides is relatively complicated. In such a case, it is hardly possible to deduce a specific mechanism from experimental data.

(3) The formed hydroxides as well as porous oxide layers on the electrode surface act as membrane inhibitors for different possible charge-transfer steps. In this case, transport processes may play an important role in the kinetics. Consequently the relatively unexplored subject of membrane inhibition complicates the electrochemical kinetics.

(4) Under these circumstances electrochemical measurements under steady state conditions do not lead to definite kinetic information [10]. Therefore, only non-steady state techniques are applicable. In such cases the most popular method is cyclic voltammetry. However, thermodynamic and kinetic data obtained by this method are known to be of a more qualitative than quantitative nature. Therefore, a correlation between the experimental results and proposed mechanisms can only be offered with certain reservations.

The aim of this work is to investigate the iron dissolution in an alkaline sulphate medium using cyclic voltammetry. Taking into account the influence of different parameters, which affect the reproducibility of the results, a comprehensive discussion is offered in order to clear up the divergencies of earlier results and to formulate the most suitable mechanisms.

2. Experimental

The cell was made of pyrex glass, was double-walled and contained electrolyte of volume about 300 cm^3. The counter and reference electrode compartments were separated from the rest of the cell by means of G4 sintered glass frits. The end of the reference electrode compartment was elongated in the form of a Luggin-capilliary, which was placed at a distance of about 0·1 cm from the surface of the working electrode.

The electrolyte consisted of 0·4 M Na_2SO_4 plus 0·1 M NaOH. The chemicals were p.a. grade (Merck) and the solutions were prepared from conductivity water.

The reference electrode was a saturated calomel electrode. The counter electrode was a platinum sheet having an area of about 10 cm^2. The working electrode was in the form of a wire (d = 0·2 cm) made from recrystallized Ommet iron*. This wire was mounted in a glass tube, whose end was sealed with high pressure polyethylene. The area of the working electrode exposed to the electrolyte was always 1 cm^2. The pre-treatment of the iron electrode started with a degreasing with acetone and washing with bidistilled water. Then the working electrode was anodically polished in a bath made from concentrated H_2SO_4, concentrated H_3PO_4 and water (1 : 3 : 1 parts by volume), at a current density of 0·8 A cm^{-2} and a temperature of T = 80 ± 5°C for about 10 min. After washing with bidistilled water and then with sulphate solution, the electrode was introduced into the cell containing the oxygen free solution.

The potential of the working electrode was controlled by a Jaissle potentiostat, type 1000 T. A function generator, developed at the Bonn University, provided the triangular potential signals. The current density-potential curves were recorded on an x–y recorder (Hewlett-Packard, type 135 M).

All experiments were carried out under an atmosphere of purified hydrogen† and at 25 ±

* Total impurities < 300 p.p.m.

† H_2 > 99·998 vol%, O_2 < 2 v.p.m.

0·1°C. All given potentials are transformed to the normal hydrogen scale.

3. Results

3.1. *Influences of the starting potential and electrode activation by cyclic prepolarization*

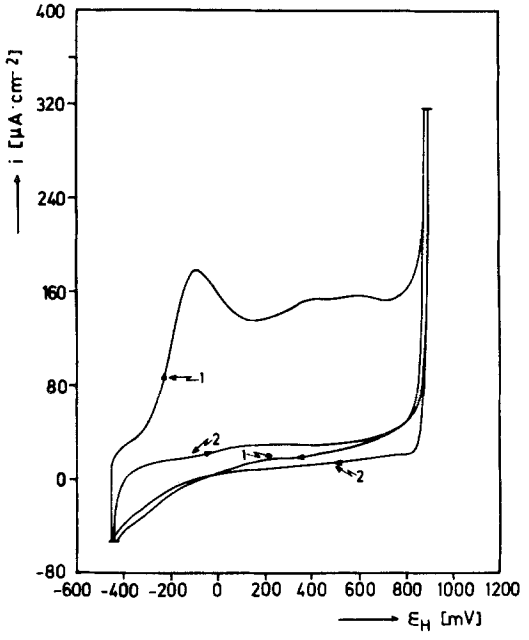

Fig. 1. Cyclic voltammetry curves starting from a potential of $\epsilon = -460$ mV. System: Fe/0·1 M NaOH + 0·4 M Na_2SO_4, $v = |d\epsilon/dt| = 40$ mV s^{-1}, $T = 298$ K
1, first sweep; 2, second sweep

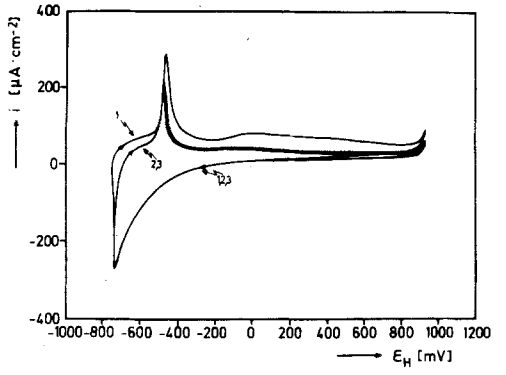

Fig. 2. Cyclic voltammetry curves starting from a potential of $\epsilon = -760$ mV. System: Fe/0·1 M NaOH + 0·4 M Na_2SO_4, $v = |d\epsilon/dt| = 40$ mV s^{-1} $T = 298$ K
1, first sweep; 2, second sweep; 3, third sweep.

Fig. 1 shows two different cyclic voltammetric current density-potential curves (voltammograms) starting from a quasi-steady-state corrosion potential of $\epsilon = -460$ mV. Curve 1 represents the first sweep and curve 2 the second one. It can be seen that both sweeps are different and obviously the forward and backward sweeps indicate irreversible processes. The influence of the sweep number can be attributed to different initial states of the electrode surface.

In Fig. 2 the electrode was pre-polarized potentiostatically at a potential of $\epsilon = -760$ mV for 10 min before starting the voltammetric sweeps. In this case the shape of the voltammogram is quite different from that in Fig. 1 and the influence of the sweep number is not so pronounced. This result indicates that the activity of the electrode surface depends also on the starting potential.

At more negative starting potentials the voltammograms are changed again. It was found that starting at a potential of $\epsilon = -1160$ mV, at which hydrogen is evolved, always led to the same shape of voltammogram as shown in Fig. 3. In this case only an influence of the sweep number on the different current maxima can be observed. This change can be attributed again to an activation process of the electrode by the cyclic polarization. During this activation process the current-density maxima 3 and 3′ are mainly influenced and increase with increasing sweep numbers from 1 to n. The other maxima 1, 2 and 2′ respectively are influenced only very little by the sweep number and are changed in the opposite direction, i.e. they decrease from 1 to n.

The sweep number n, after which no remarkable change in the voltammogram can be observed, depends on the scanning rate and corresponds to a maximum activity of the electrode surface.

On interrupting the cyclic voltammetry and keeping the electrode potentials at values between $\epsilon = -969$ and $\epsilon = -1160$ mV for a relatively long time (1–2 h), no change in the activity of the

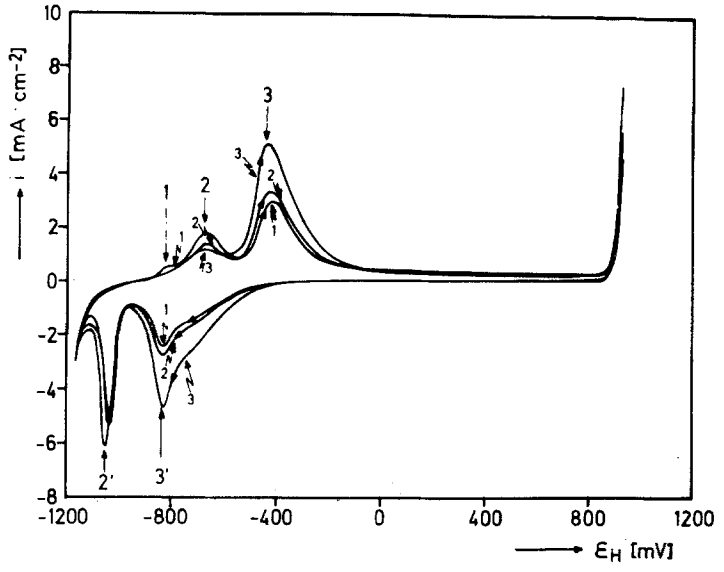

Fig. 3. Cyclic voltammetry curves starting from a potential of $\epsilon = -1160$ mV showing the dependence of activation process on sweep number. System: Fe/0·1 M NaOH + 0·4 M Na_2SO_4, $\nu = |d\epsilon/dt| = 40$ mV s^{-1} $T = 298$ K
Small numbers. 1, first sweep; 2, second sweep; 3, eighth sweep. The large numbers (1, 2, 3, 3′, and 2′) correspond to current maxima.

electrode surface was recognized, i.e. the sweep after the interruption corresponds exactly to the sweep before. The following experiments were carried out at constant maximum activity of the electrode surface.

3.2. *Correlation between anodic and cathodic current maxima*

In Fig. 4 a cyclic voltammogram at maximum activity of the electrode surface is shown. It can be seen that the anodic sweep includes three maxima 1, 2 and 3.

As mentioned above, the maximum 1, disappears after the first sweep. The electrode potentials of the anodic maxima 1, 2 and 3 are $\epsilon_{max,\,1} = -810$ mV, $\epsilon_{max,\,2} = -660$ mV and $\epsilon_{max,\,3} = -440$ mV respectively. The current after passing maximum 3 decreases to a relatively small value ($\sim 150\ \mu A\ cm^{-2}$) and remains constant over a potential of almost 1 *V* before it increases abruptly. This last increase corresponds to the oxygen evolution reaction.

The cathodic sweep shows two maxima 3′ and 2′, which appear at potentials of $\epsilon_{max,\,3'} = -820$ mV and $\epsilon_{max,\,2'} = -1040$ mV respectively. After maximum 2′ there is a cathodic current increase corresponding to the hydrogen evolution reaction. The correlation between the anodic and cathodic maxima has been carried out either by starting at different potentials, as illustrated in Figs. 5 and 6, or by restricting the anodic sweep to a different potential range as shown in Figs. 7 and 8.

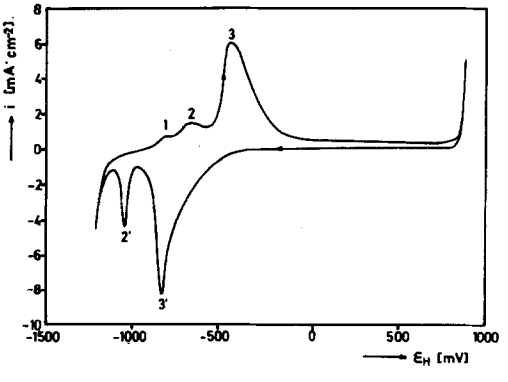

Fig. 4. Cyclic voltammetry curve at the maximum activation, starting from a potential of $\epsilon = -1200$ mV. System: Fe/0·1 M NaOH + 0·4 M Na_2SO_4, $\nu = |d\epsilon/dt| = 40$ mV s^{-1}, $T = 298$ K

By comparing the different curves, it is clear that a correlation exists between the maxima 2 and 2′, and 3 and 3′, respectively.

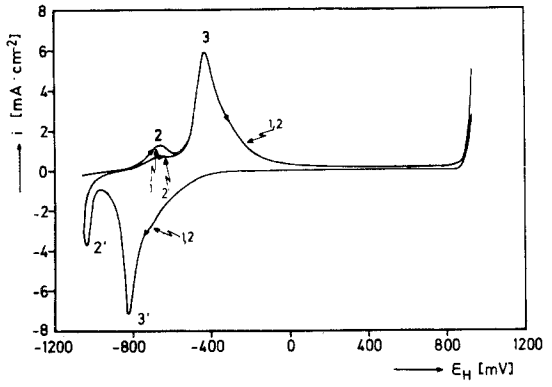

Fig. 5. Cyclic voltammetry curves at the maximum activation, starting from a potential of $\epsilon = -1050$ mV. System: Fe/0·1 M NaOH + 0·4 M Na_2SO_4, $\nu = |d\epsilon/dt| =$ 40 mV s^{-1}, $T = 298$ K

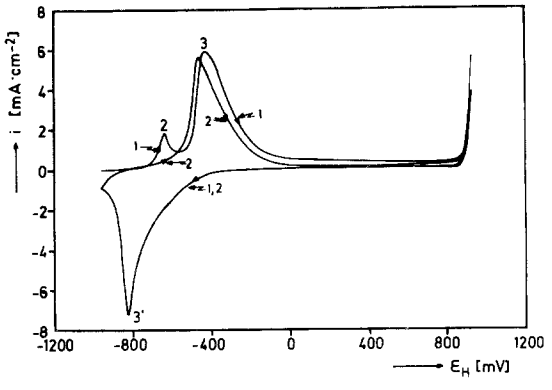

Fig. 6. Cyclic voltammetry curves at the maximum activation, starting from a potential of $\epsilon = -950$ mV. System: Fe/0·1 M NaOH + 0·4 M Na_2SO_4, $\nu = |d\epsilon/dt| =$ 40 mV s^{-1}, $T = 298$ K

3.3. *Influence of sweep rate*

The influence of the sweep rate ν on the peak current densities i_p of the maxima 2, 2′ and 3, 3′ is illustrated in Fig. 9, whereby $\log |i_p|$ versus $\log (|d\epsilon/dt|)$ is plotted. A linear relationship is obtained for all maxima with the slope

$$\left(\frac{\partial \log |i_p|}{\partial \log \nu}\right)_{a_i,\ T} = 0{\cdot}85 \pm 0{\cdot}05.$$

The variation of the peak potentials with the sweep rate is about 40–50 mV per decade. With increasing sweep rate, the anodic maxima 2 and 3 are shifted to more positive potentials, whereas the cathodic ones 2′ and 3′ are shifted in the negative direction.

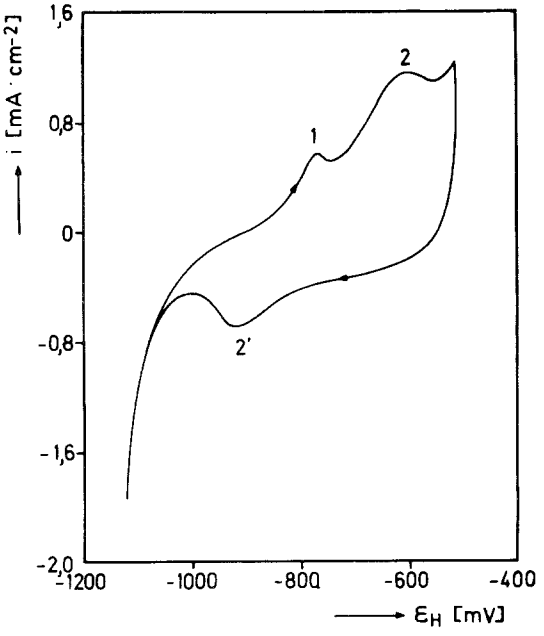

Fig. 7. Cyclic voltammetry curve at the maximum activation, reversed at the potential $\epsilon = -540$ mV. System: Fe/0·1 M NaOH + 0·4 M Na_2SO_4, $\nu = |d\epsilon/dt| =$ 40 mV s^{-1}, $T = 298$ K

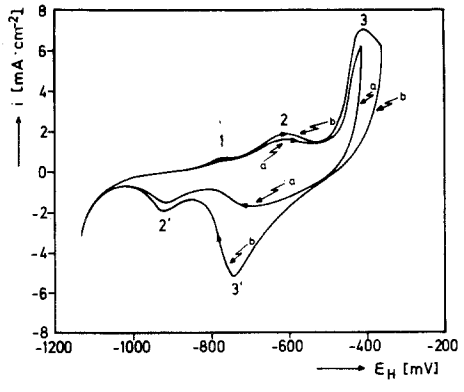

Fig. 8. Cyclic voltammetry curves at the maximum activation, reversed at the potential $\epsilon = -440$ mV (curve *a*) and $\epsilon = -309$ mV (curve *b*). System: Fe/0·1 M NaOH + 0·4 M Na_2SO_4, $\nu = |d\epsilon/dt| = 40$ mV s^{-1}, $T = 298$ K

3.4. *Oxygen evolution and reduction*

If oxygen evolution takes place to some extent during the anodic sweep, then in the following cathodic sweep an additional maximum can be observed, as is demonstrated in Fig. 10. The potential corresponding to this maximum is more positive than that of maximum 3′: $\epsilon_{max} =$

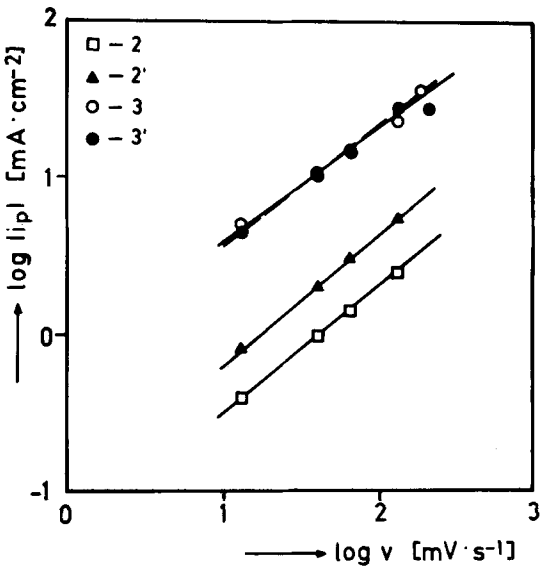

Fig. 9. The influence of the sweep rate, $\nu = |d\epsilon/dt|$, on the current maxima. System: Fe/0·1 M NaOH + 0·4 M Na_2SO_4, $T = 298$ K

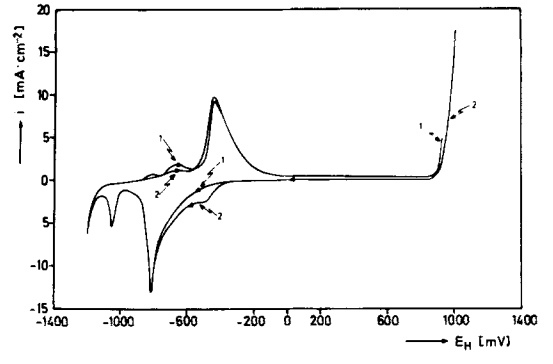

Fig. 10. Cyclic voltammetry curves showing the oxygen reduction maximum. System: Fe/0·1 M NaOH + 0·4 M Na_2SO_4, $\nu = 40$ mV s^{-1}, $T = 298$ K

−460 mV. Its magnitude is dependent both on the extent of oxygen evolution and the degree of stirring of the electrolyte solution. These two parameters influence the magnitude of this maximum in opposite ways i.e. it increases with the extent of oxygen evolution and decreases if the stirring of the solution is increased.

4. Discussion

The initial state of the electrode surface seems to be an important factor influencing the form of the current density-potential curves. If the experiments are started at electrode potentials between $\epsilon = -460$ mV and $\epsilon = -1060$ mV, then the electrode surface is covered with an oxide film. This film can arise either by oxidation of the electrode surface in the atmosphere before dipping it in the electrolyte or from the corrosion processes taking place at the open circuit potentials. Consequently in such cases the obtained voltammograms will be a function of this indefinite starting condition [11]. Figs. 1 and 2 illustrate this behaviour.

At a starting potential of $\epsilon \leqslant -1160$ mV, hydrogen evolution occurs. In this case the oxide film on the electrode surface can be totally reduced and a reproducible initial state of the electrode surface is achieved. This starting condition is a necessary requirement for the comparison of different results [12, 14, 15]. Under this condition the voltammograms are characterized as follows.

(1) The number of anodic and cathodic maxima is constant and the corresponding peak potentials are very reproducible. In Fig. 4 it is shown that there exist three anodic and two cathodic maxima. This is in accordance with the recent results of McDonald and Owen [14]. However, Cnobloch *et al.* [15] obtained an additional peak in the anodic as well as in the cathodic sweep.

(2) The peak currents depend on the sweep number in a different way, as can be seen from Fig. 3. This can be attributed to a change in the activation state of the electrode surface.

(3) The charge amount q_a, integrated for the anodic sweep under maximum activation conditions for the total investigated potential range, is nearly equal to q_c obtained for the cathodic sweep. Also these charge amounts are independent of the scanning rate. The calculated q-values are of the magnitude of about 40 mC cm^{-2} and consequently indicate the formation of multi-atomic oxide layers on the electrode surface.

The correlation between the experimentally observed maxima and the electrode processes taking place is relatively difficult, because for this system sufficient electrochemical kinetic information cannot be obtained. However, the following correlations will be assumed:

(1) The maximum 1 can be attributed to the oxidation of hydrogen, which is adsorbed on the electrode surface as well as absorbed in the metal

lattice. This conclusion results from the following observations:

The maximum 1 appears only if hydrogen evolution on the electrode surface takes place previously. This can be seen by comparing Figs. 4–7. Moreover, this maximum 1 decreases with increasing sweep number, which is demonstrated in Fig. 3.

This correlation is in agreement with the interpretation of Cnobloch *et al.* [15]. On the other hand, McDonald and Owen [14] attributed this maximum to the oxidation of iron to $Fe(OH)_2$.

(2) The maxima 2, 2′ are certainly due to iron electrode processes. Taking into account the thermodynamic stability ranges, then the reactions, which can take place in the potential range of maxima 2 and 2′ respectively may be represented as follows:

$$Fe + 2\,OH^- \rightleftharpoons [Fe\,(OH)_2]_{ads} + 2\,e^- \quad (1)$$

This overall reaction will occur in different steps. According to Kabanov *et al.* [5] the following mechanism can be assumed:

$$Fe + OH^- \rightleftharpoons (FeOH)_{ads} + e^- \quad (2)$$

$$(FeOH)_{ads} + OH^- \rightleftharpoons (FeO)_{ads} + H_2O + e^- \quad (3)$$

$$(FeO)_{ads} + OH^- \rightleftharpoons HFeO_2^- \quad (4)$$

$$HFeO_2^- + H_2O \rightleftharpoons Fe(OH)_2 + OH^- \quad (5)$$

whereby step 3 is rate determining. The following electrochemical data under steady state conditions can be derived from this mechanism for the anodic process: a Tafel slope of $b_+ = +40$ mV ($T = 298$ K, $\alpha = 0{\cdot}5$) and an electrochemical reaction order, related to the pH, of $n_{+,pH} = +2$. From the measurements of Kabanov *et al.* [5] only the Tafel slope was confirmed. Therefore other possibilities may be considered taking into account the iron dissolution mechanisms in acid media [17]:

$$Fe + OH^- \rightleftharpoons (FeOH)_{ads} + e^- \quad (2)$$

$$(FeOH)_{ads} \rightleftharpoons FeOH^+ + e^- \quad (6)$$

$$FeOH^+ + 2\,OH^- \rightleftharpoons HFeO_2^- + H_2O \quad (7)$$

$$HFeO_2^- + H_2O \rightleftharpoons [Fe\,(OH)_2]_{ads} + OH^- \quad (8)$$

In this case the anodic electrochemical reaction order decreases to $n_{+,pH} = +1$. The steps 7 and 8 can be replaced by a single equilibrium:

$$FeOH^+ + OH^- \rightleftharpoons [Fe\,(OH)_2]_{ads} \quad (9)$$

In both mechanisms the adsorbed species $Fe[(OH)_2]_{ads}$ is formed via the soluble bihypoferrite-ion $HFeO_2^-$. However, the direct formation of the adsorbed species $[Fe(OH)_2]_{ads}$ by a topochemical reaction cannot be excluded:

$$Fe + OH^- \rightleftharpoons (FeOH)_{ads} + e^- \quad (2)$$

$$(FeOH)_{ads} + OH^- \rightleftharpoons [Fe(OH)_2]_{ads} + e^- \quad (10)$$

This mechanism is very similar to the steps 2 and 3 of the mechanism postulated by Kabanov. Also the anodic kinetic data are the same. A following chemical dissolution of the intermediate $[Fe(OH)_2]_{ads}$ can take place in concentrated alkaline solutions accordingly to step 4:

$$[Fe\,(OH)_2]_{ads} + OH^- \rightleftharpoons HFeO_2^- + H_2O \quad (11)$$

Another possibility is that step (10) is in electrochemical equilibrium and occurs in parallel with one of the other postulated mechanisms. This would agree with the results of theoretical considerations of the iron dissolution mechanism in weak acid solutions in the potential range between the active and passive state [18]. Moreover, the measured q_{a-} and q_{c-} values in the potential range of the maxima 2 and 2′ indicate the formation and reduction respectively of multilayer oxide films. Therefore the end product of oxidation in this step will not be $[Fe\,(OH)_2]_{ads}$, but a three-dimensional oxide film:

$$[Fe\,(OH)_2]_{ads} \rightleftharpoons Fe\,(OH)_2\text{-oxide phase} \quad (12a)$$

or rewritten

$$Fe_s[Fe(OH)_2]_{ads} + 2OH^- \rightleftharpoons 2\,Fe(OH)_2\text{-oxide phase} + 2\,e^- \quad (12b)$$

whereby Fe_s is a substrate atom. This formulation is used in order to explain the three-dimensional film formation.

A distinction between the different mechanisms is not yet possible due to insufficient kinetic data for iron dissolution in alkaline media.

The given interpretation of maxima 2 and 2′ is in accordance with that of Cnobloch *et al.* [15], but is in contradiction to that of McDonald and

Owen [14], who correlate this maxima with the formation and reduction respectively of Fe_3O_4.

(3) The maxima 3 and 3′ represent the further oxidation of iron species to a higher valency state. Different possibilities exist. According to Kabanov *et al.* [5]

$$(FeOH)_{ads} + OH^- \rightleftharpoons (FeO, OH)_{ads} + H^+ + 2\,e^- \quad (13)$$

This reaction step is a topochemical one. Cnobloch *et al.* [15] include two different ways. A topochemical step as follows

$$3[Fe(OH)_2]_{ads} + 2\,OH^- \rightleftharpoons Fe_3O_4 + 4\,H_2O + 2\,e^- \quad (14)$$

as well as a route via the solution phase

$$HFeO_2^- \rightleftharpoons FeO_2^- + H^+ + e^- \quad (15)$$

followed by

$$HFeO_2^- + 2\,FeO_2^- + H_2O \rightleftharpoons Fe_3O_4 + 3\,OH^- \quad (16)$$

The authors assume that the second way is energetically favoured compared to the first one. This conclusion arises on the basis of the two different current peaks formed anodically as well as cathodically in this potential range. The appearance of two different maxima can be attributed to the highly active electrode material which was used as well as to the relatively highly concentrated alkaline media.

However, McDonald and Owen [14] have already correlated maxima 2 and 2′ with the formation of Fe_3O_4 according to step 14. Therefore they assume the formation of γ-Fe_2O_3 in the potential range of maxima 3 and 3′ by the parallel reactions:

$$2\,Fe + 6\,OH^- \rightleftharpoons \gamma - Fe_2O_3 + 3\,H_2O + 6\,e^- \quad (17)$$

This reaction can take place in two steps:

$$Fe + 2\,OH^- \rightleftharpoons [Fe(OH)_3]_{ads} + 3\,e^- \quad (18)$$

$$2[Fe(OH)_3] \rightleftharpoons \gamma - Fe_2O_3 + 3\,H_2O \quad (19)$$

The present investigation shows (see Fig. 3) that the maxima 3 and 3′ increase with increasing sweep number, whereas maxima 2 and 2′ decrease. Therefore the reactions taking place at maxima 3 and 3′ are parallel to those occurring at maxima 2 and 2′. This is in agreement with the statement of McDonald and Owen [14]. The formation of multilayers of iron oxides in a higher valency state can be formulated as follows:

$$Fe_s + 2\,Fe(OH)_2\text{-oxide phase} + 4\,OH^- \rightleftharpoons Fe_3O_4 + 4\,H_2O + 4\,e^- \quad (20)$$

followed by the transformation reaction

$$Fe_s + Fe_3O_4 + 4\,OH^- \rightleftharpoons 2\gamma - Fe_2O_3 + 2\,H_2O + 4\,e^- \quad (21)$$

Both reactions are topochemical. In the present experiments no splitting of the maxima 3 and 3′ respectively was observed. This is in agreement with the results of McDonald and Owen [14]. Probably the reason for this behaviour is due to the smooth electrodes and relatively low concentration of OH^- ions which were used, compared to the conditions of Cnobloch *et al.* [15]. Therefore the formulation of iron surface oxides via the solution phase according to steps (15) and (16) diminishes. This is in agreement with the results of Armstrong *et al.* [12], who did not observe the participation of soluble species in the electrode reaction under such conditions.

The above-mentioned dependence of the activation state of the electrode on the sweep number can be explained by the three-dimensional growth processes, a change of the roughness factor and a hindrance of diffusion steps in the solid oxide film. The last phenomenon could explain the so-called maximum activity state of the electrode in terms of limiting diffusion conditions.

The obtained result for the relationship between the peak current densities and the scanning rate is in satisfactory agreement with the theoretical value of $(\partial \log i_p/\partial \log \nu)_{a_i,T} = +1$ derived by Srinivasan and Gileadi [19] for electrode reactions involving adsorbed species.

Acknowledgements

The authors thank the 'Arbeitsgemeinschaft Industrieller Forschungsvereinigungen (AIF)' and the 'Max-Buchner-Forschungsstiftung' in Germany for financial support of this work. One of us (D.G.) is grateful for sabbatical leave.

References

[1] J. O'M. Bockris and A. K. N. Reddy, 'Modern Electrochemistry', Vol. 2, Plenum Press, New York (1970).

[2] H. Cnobloch, G. Siemsen and F. v. Sturm, *Siemens Forsch. u. Entwickl. Ber.* **1** (1972) 221.

[3] D. A. Vermilya, Anodic Films, in 'Advances in Electrochemistry and Electrochemical Engineering', Vol. 3, ed. P. Delahay and C. W. Tobias, Interscience Publ., New York (1963).

[4] U. R. Evans, 'The Corrosion and Oxidation of Metals', Vol. 1, Arnold London (1968).

[5] B. Kabanov, R. Burstein and A. Frumkin, *Discuss. Faraday Soc.* **1** (1947) 259.

[6] K. G. Weil, *Z. Elektrochem.* **62** (1958) 638.

[7] T. Hurlen, *Electrochim. Acta* 8 (1963) 609.

[8] A. J. Salkind, C. N. Venuto and S. U. Falk, *J. Electrochem. Soc.* **111** (1964) 493.

[9] C. L. Foley, J. Kruger and C. J. Bechtold, *ibid* **114** (1967) 994.

[10] C. M. Schephard and S. Schuldiner, *ibid* **115** (1968) 1124.

[11] S. Asakura and K. Nobe, *ibid* **118** (1971) 536.

[12] R. D. Armstrong and I. Baurhoo, *J. Electroanalyt. Chem. Interfacial Electrochem.* **34** (1972) 41.

[13] G. J. Bignold, *Corrosion Sci.* **12** (1972) 145.

[14] D. D. McDonald and D. Owen, *J. Electrochem. Soc.* **120** (1973) 317.

[15] H. Cnobloch, D. Gröppel, W. Nippe and F. v. Sturm, *Chemie-Ingenieur-Technik* **45** (1973) 203.

[16] D. Geana, A. A. El Miligy and W. J. Lorenz, *Corrosion Sci.* **13** (1973) 505.

[17] F. Hilbert, Y. Miyoshi, G. Eickorn and W. J. Lorenz, *J. Electrochem. Soc.* **118** (1971) 1919, 1927.

[18] A. A. El Miligy, D. Geana and W. J. Lorenz, submitted to *Electrochim. Acta.*

[19] S. Srinvasan and E. Gileadi, *Electrochim Acta* **11** (1966) 321.